

Dynamical Mean Field Theory of Double Perovskite Ferrimagnets

K. Phillips¹, A. Chattopadhyay², A. J. Millis³

¹*Department of Physics and Astronomy, Rutgers University
136 Frelinghuysen Rd, Picataway, NJ 08854*

²*IBM Almaden Research Center
650 Harry Road, San Jose, CA*

³*Department of Physics, Columbia University
538 West 120th Street, NY, NY, 10027*

(Dated: May 22, 2022)

The dynamical mean field method is used to analyze the magnetic transition temperature and optical conductivity of a model for the ferrimagnetic double perovskites such as Sr_2FeMoO_6 . The calculated transition temperatures and optical conductivities are found to depend sensitively on the band structure. For parameters consistent with local spin density approximation band calculations, the computed transition temperatures are lower than observed, and in particular decrease dramatically as band filling is increased, in contradiction to experiment. Band parameters which would increase the transition temperature are identified.

PACS numbers:

I. INTRODUCTION

The calculation of non-zero-temperature and dynamical properties, such as magnetic transition temperatures and conductivities, is a long-standing and difficult problem in materials theory, but one for which the recent theoretical development of the 'dynamical mean field' method¹ offers a promising avenue for progress. This method, which allows an exact (in principle) treatment of local correlations has been recently used in combination with 'ab initio' band calculations to estimate the transition temperatures of Fe and Ni ⁵, and in combination with a tight binding parametrization of band theory to elucidate the physics of the 'colossal' magnetoresistance manganites^{2,6,7,8} and models of magnetic semiconductors^{3,4}.

In this paper we apply the method to study ferrimagnetic members of the 'double perovskite' family of materials. These are compounds of chemical formula $ABB'O_6$, with A an alkaline earth such as Sr , Ca or Ba , and B, B' two different transition metal ions. In the ferrimagnets of present interest the B site is occupied by Fe and B' site by a member of the $4d$ or $5d$ transition metal series such as Re or Mo . The double perovskite family of materials have long been known⁹ but the ferrimagnetic members listed above have become the subject of recent interest^{10,11,12,13,15} because they seem to be to be metallic (except perhaps in the Ca case¹³ ferrimagnets with magnetic transition temperatures greater than room temperature and apparently highly spin-polarized conduction bands, raising the possibility of interesting device applications as 'spin valves'¹⁶, elements in magnetic information storage systems¹⁷ and as sources of spin polarized electrons for spintronic applications¹⁸.

The materials are also of fundamental interest, because their physics and materials science are far from understood. For example, apparently minor changes

in chemical composition or processing conditions can change the electrical behavior from metallic to insulating, or the magnetic transition temperature from $400K$ to $200K$. More generally, the materials provide examples of novel behaviors associated with partial filling of transition metal $4d/5d$ shells, which have been little studied in comparison to the $3d$ transition metal series¹⁹. Further, the specific materials we wish to study are believed to be half metallic ferrimagnets, but the obvious strong interaction which could give rise to half metallicity (a Hunds coupling on the Fe) exists on only one of the two sites, unlike the situation in the somewhat analogous CMR materials. Thus behavior arising from the interplay of magnetic order and carrier motion may be different. Finally, the origin of the magnetism is not settled. A natural guess is that it is due to the strong Hunds coupling on the Fe site, but other interactions have been proposed to be important¹²

In this paper we present a model for the low (less than, say $3eV$) lying electronic states, which are important for transport and magnetism. Our model consists of a tight binding description of the bands, which we derive from previously published first principles calculations^{11,12} and general arguments, and a local interaction (namely a Hunds coupling on the Fe site). The key physical assumption made in our model is that the magnetism is driven by the strong Hunds coupling on the Fe site. Important technical issues include the two dimensional nature of the underlying band structure and the multi-orbital nature of the material. We solve the model in the dynamical mean field approximation, and from our solution determine the magnetic transition temperature and optical conductivity, and attempt to determine the general materials aspects which control T_c . This paper supercedes a previous paper¹⁴, in which the model Hamiltonian used did not provide an adequate approximation to the underlying band structure.

II. MATERIAL AND MODEL

A. Material

Double perovskite systems form in the $ABB'O_6$ crystal structure which generalizes the ABO_3 perovskite structure familiar from ferroelectrics, high temperature superconductors and the 'colossal' magnetoresistance rare earth manganites by having two different B site ions. In the double perovskite materials of interest here, A is an alkaline earth such as Sr , Ca or Ba and the B, B' sites form a rocksalt structure, i.e. a simple cubic lattice with a doubled unit cell and one sublattice occupied by Fe and the other by a transition metal from the $4d$ or $5d$ series such as Mo or Re . The crystal fields and atomic energetics are such that the formal valences correspond to Fe with a half filled, maximally polarized d -shell while the Mo/Re has one or two d electrons distributed over the t_{2g} levels^{9,11,12}. We will focus on electronic states arising from the transition metal d -levels.

B. Hamiltonian

1. Overview

The Hamiltonian describing the low lying, electronically active degrees of freedom may be written as the sum of a 'hopping' part arising from the band structure and an interaction part:

$$H = H_{band} + H_{int} \quad (1)$$

The relevant portions of the calculated^{11,12} band structure involve three bands (degenerate in the ideal double perovskite structure) arising from the three transition metal t_{2g} levels $d_{xy,yz,xz}$. To a high degree of accuracy these three bands do not hybridize with each other and the physics is therefore described by a three-fold degenerate tight binding model. The planar character of the t_{2g} levels implies that the tight binding model has an interesting two dimensionality, which may be summarized as follows. The d_{xy} orbital on a Fe site hybridizes via a matrix element t_1 with the d_{xy} levels on the four nearest neighbor (Mo/Re), sites *in the same plane* and via a much smaller matrix element t_3 to the four nearest Fe ions also in the same plane. The hopping in the third direction is negligible, because of the planar character and xy orbital symmetry of the d_{xy} wave function. The d_{xy} orbital on a Mo/Re site hybridizes with the four in-plane near neighbor Fe sites via the same hopping matrix element t_1 and with the four in-plane second nearest neighbor (Mo/Re) sites, via another matrix element t_2 , which is not particularly small, because of the more spatially extended character of the d -electrons in $4d/5d$ orbitals. Further neighbor hoppings are also found to be important in other t_{2g} -based $4d$ systems such as Sr_2RuO_4 ²⁰.

It is natural to assume that the magnetic character of the material derives from the strongly magnetic nature

of the Fe ion and we therefore assume that the dominant interaction arises from the strong atomic Hunds coupling of the Fe .

2. Hopping Hamiltonian

To write the Hamiltonian explicitly we focus the cubic lattice of B, B' sites in the underlying single perovskite structure, labelling these sites by i and the operator creating an electron into orbital $a(= xy, yz, xz)$ and spin σ by $c_{a,i,\sigma}^+$. Although we refer to this orbital as a ' d -orbital' it in fact represents a hybrid, composed mainly of transition metal d and oxygen p orbitals, of the correct local symmetry. We introduce a nearest neighbor ($Fe \leftrightarrow Mo/Re$) hopping t_1 and two second neighbor (same sublattice) hoppings t_2 and t_3 representing $Mo - Mo$ or $Fe - Fe$ hoppings respectively. As noted above we expect that t_2 corresponding to $Mo - Mo$ hopping is relatively large, because of the larger spatial extent of the $4d/5d$ orbitals while t_3 is essentially negligible. To obtain the conductivity we couple in the electric field by using a vector potential and the Peierls phase ansatz. This approximation has been shown to be accurate in other transition metal oxide contexts^{22,23}. Thus the hopping portion of the Hamiltonian is the sum of three identical tight binding models, one for each orbital. The Hamiltonians take the general form (note that the first sum runs over all lattice sites, the second over the B' (non-Fe) and the third over the B (Fe) sites, while δ_a labels the in-plane direction relevant to orbital a and we have set the electric charge e and the speed of light c equal to unity)

$$\begin{aligned} H_{band} = & - \sum_{a,i,\delta_a,\sigma} (t_{1,a} e^{i\mathbf{A}\cdot\delta_a} c_{a,i,\sigma}^+ c_{a,i+\delta_a,\sigma} + H.c.) \\ & - \sum_{a,i \in B', \delta'_a} (t_{2,\alpha} e^{i\mathbf{A}\cdot\delta'_a} c_{i,a,\sigma}^+ c_{i+\delta'_a,a,\sigma} + H.c.) \quad (2) \\ & - \sum_{a,i \in B, \delta'_a} (t_{3,\alpha} e^{i\mathbf{A}\cdot\delta'_a} c_{i,a,\sigma}^+ c_{i+\delta'_a,a,\sigma} + H.c.) \end{aligned}$$

H_{band} implies an interesting band structure, which is most plainly revealed by writing H_{band} in momentum space in a matrix notation where the upper left entry corresponds to Fe and the lower right to Mo , thus if $A = 0$ we have, for the xy orbitals

$$H_{band,xy}[A = 0] = \begin{pmatrix} 0 & -2t_1 (\cos p_x + \cos p_y) \\ -2t_1 (\cos p_x + \cos p_y) & -4t_2 \cos p_x \cos p_y \end{pmatrix} \quad (3)$$

where we have set the $Fe - Mo$ distance to unity and the momenta are restricted to the reduced Brillouin zone $|p_x| + |p_y| < \pi$.

3. Interaction

The most important interaction effect constrains the occupancy of the B (Fe) site. The formal valence of Fe is d^5 and the strong Hunds coupling characteristic of Fe (and found in the local spin density approximation to band theory) means that in the d^5 configuration all of the Fe d -electrons are aligned, leading to a filled, completely spin-polarized d -shell. Two charge fluctuation processes are possible: $Fed^5 \leftrightarrow Fed^4$ or $Fed^5 \leftrightarrow Fed^6$. The strongly stable nature of the filled d -shell implies that the $d^5 - d^6$ process is dominant. To express this physics we introduce a strong Hunds coupling on the B (Fe) site, expressing the fact that in the ground state the Fe is in the d^5 maximal spin configuration, and an energy splitting parameter Δ expressing the differing electronegativities of the B and B' sites. Thus we write

$$H_{int} = -J \sum_{a,i \in B\alpha\beta} \vec{S}_i \cdot \vec{c}_{a,i,\alpha}^+ \vec{\sigma}_{\alpha\beta} c_{a,i,\beta} + \sum_{a,i \in B',\sigma} \Delta^a c_{a,i,\sigma}^+ c_{a,i,\sigma} \quad (4)$$

For the calculations presented in this paper we will specialize to cubic symmetry, so the Δ are the same for all three orbitals, but this restriction may easily be lifted. The energy scale relevant for the $Fed^5 \leftrightarrow Fed^6$ valence fluctuation is $J - \Delta$. Examination of published band structures^{11,12} indicates that $J - \Delta \sim 1eV$ while the $d^5 \leftrightarrow d^4$ process has a much larger energy of $|J + \Delta| \geq 5eV$. In a fully spin polarized ground state, the interaction terms simply become level shifts, $\Delta_{maj} = J + \Delta$ and $\Delta_{min} = -J + \Delta$ for the majority and minority spin bands. Transitions onto the majority-spin Fe orbital involve very large energies, so to simplify the calculations at $T > T_c$ we will take the limit $J + \Delta \rightarrow \infty$ with $J - \Delta$ fixed. We henceforth refer to the quantity $J - \Delta$ as Δ . Because the local spin density approximation may not be accurate for strongly interacting systems such as the double perovskites, we will consider a range of Δ here.

Other authors¹⁵ have argued that an additional Hunds-type coupling on the B' site is important. Technical limitations prevent us from treating such an interaction accurately, so we do not include it here.

4. Discussion: $T=0$ Band structure, ferromagnetic case

Eq 3 may be thought of as describing two bands of electrons: one on the Fe sites, with 'intrinsic' bandwidth set by t_3 and one on the non- Fe sites, with 'intrinsic' bandwidth set by t_2 . The two bands hybridize via the overlap $-2t_1(\cos p_x + \cos p_y)$. We see immediately that the hybridization vanishes along the line $\cos p_x + \cos p_y = 0$ which also contains the van Hove points $0, \pi$ and $\pi, 0$ at which the density of states of the two individual bands diverges. Near these points a complicated structure including divergences in the density of states is expected.

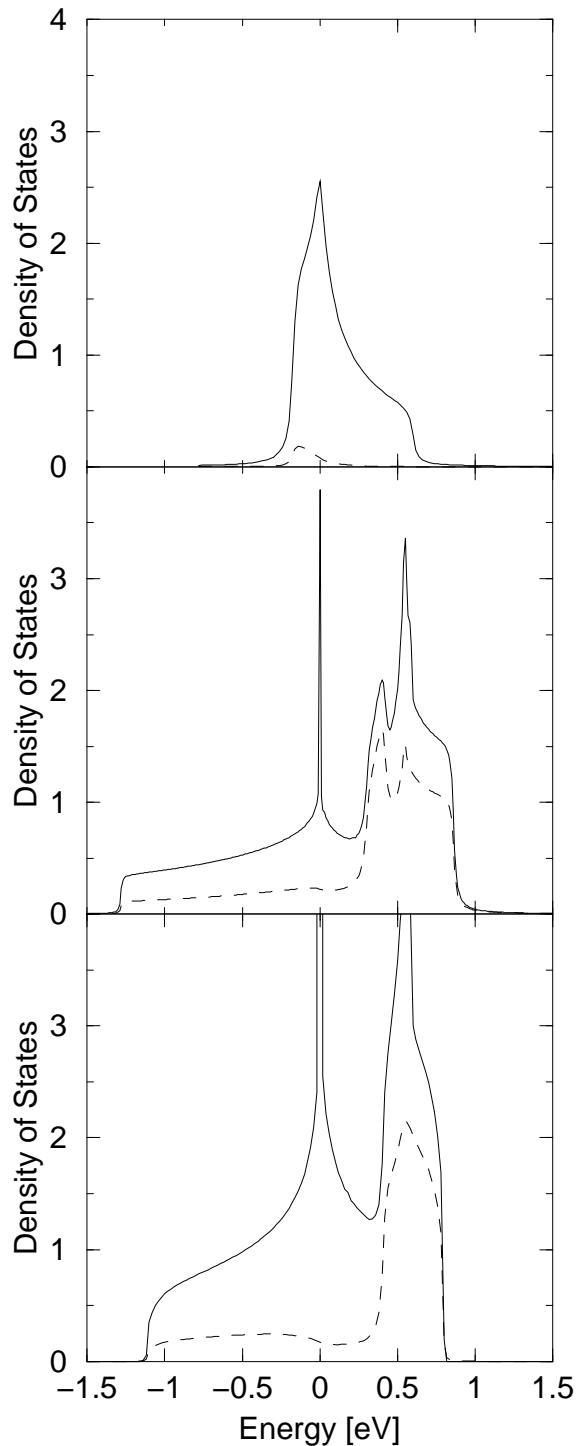


FIG. 1: Total (solid line) and Fe -projected (dashed line) densities of states computed using tight binding parameters $t_1 = 0.25$ eV, $t_2 = 0.15$ eV, $t_3 = 0.03$ eV. Top panel: $T = 0$ majority spin density of states using $\Delta_{maj} = -2.5$ eV Middle panel: $T = 0$ minority spin density of states computed from Eq. 3 with $\Delta_{min} = 0.3$ eV. Lowest panel: total (both spins) density of states at $T > T_c$ computed as described in section III.

The full density of states and the projection of this density of states onto the Fe orbitals are shown in the upper panels of Fig. 1 for parameters $t_1 = 0.25$ eV, $t_2 = 0.15$ eV, $t_3 = 0.03$ eV (note that most of the majority spin Fe density of states is at a low energy outside the range of this plot). Comparison of this density of states to the published band theory results^{11,12} shows that these parameters reproduce the band density of states accurately. The main difference is that if the J and Δ are adjusted to correctly reproduce the minority spin band, then the upper (non- Fe -portion) of the majority spin band is positioned about 0.5 eV too low in energy. The extra shift in the majority spin Mo orbitals must be attributed to a Hunds coupling on the non- Fe site, not included here.

The two features seen in our calculated density of states near 0.5 eV arise from states in the vicinity of the van Hove points $(0, \pi)$ and $(\pi, 0)$ where the hybridization vanishes and the B and B' sites have energy $\Delta + 4t_3 \simeq 0.4$ eV and $4t_2 \approx 0.6$ eV respectively, whereas the peak at $\omega = 0$ arises from the van Hove point $(\pi/2, \pi/2)$ of the B' (non- Fe) band, where as noted above the hybridization to the Fe vanishes.

Formal valence arguments indicate that the material contains one or two d-electrons beyond the filled shell $Fe - d^5 Re/Mo - d^0$ configuration. Fig 1 shows that for the band theory parameters, these carriers go into states with only a small admixture of Fe . The physics behind this result is that for this sign of t_2 the strongly hybridized states near $p_x = p_y = 0$ are at the bottom of the band described by the t_2 -only term in H_{band} , and are pushed further away from the Fe states by usual level repulsion, leading to a mainly non- Fe character of the lowest states. For $n - 1$ (Re) only the minority spin band is occupied (the majority spins occupy low-lying Fe states off of the plotted scale). However, for $n = 2$ within this approximation, chemical potential is $\mu_2 \approx 0$ and the majority spin band is somewhat occupied, so the material is not a 'half-metal' in this approximation. These features will be seen to be of importance for the calculated transition temperature and optical conductivity.

It is interesting to consider a contrasting set of parameters, for which the level repulsion argument works in the opposite manner. If t_2 has an unphysical (negative) sign and Δ is near 0 then the low lying states of the t_2 -band do not mix with the Fe states, which are pushed downwards by hybridization with the higher-lying Re/Mo levels, leading to low-lying states of mainly Fe character, as shown in Fig 2.

C. Conductivity

The current operator $\hat{J} = \delta H / \delta A^{23}$. For electric field in the x direction the xy and xz orbitals contribute, thus $J_x = J_{x,xy} + J_{x,xz}$ with δ_x the lattice vector in the x direction and δ' labelling the four 'second neighbor' lattice vectors ($\delta' = \pm(\delta_x \pm \delta_y)$) so by expanding Eq 2 in

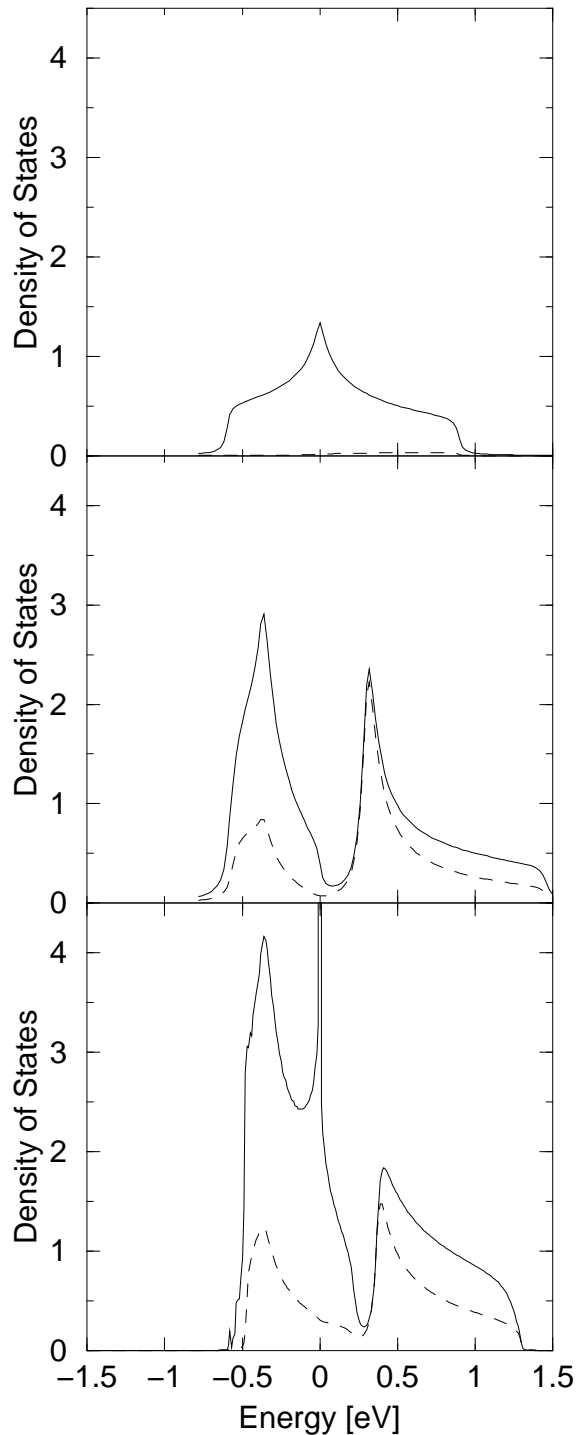


FIG. 2: Total (solid line) and Fe -projected (dashed line) densities of states computed using alternative tight binding parameters $t_1 = 0.25$ eV, $t_2 = -0.15$ eV, $t_3 = 0.03$ eV. Top panel: $T = 0$ majority spin density of states computed from Eq. 3 using $\Delta_{maj} = -2.5$ eV. Middle panel: $T = 0$ minority spin density of states computed from Eq. 3 with $\Delta_{min} = 0.3$ eV. Lowest panel: total (both spins) density of states at $T > T_c$ computed as described in section III.

powers of A we obtain

$$\begin{aligned}
J_{x,xy}(A) = & \\
& - \sum_{i,\pm\delta_x,\sigma} (i\delta_x t_{1,a} e^{i\mathbf{A}\cdot\delta} c_{xy,i,\sigma}^+ c_{xy,i+\delta_x,\sigma} - H.c.) - \\
& \sum_{i\in B',\delta'_a} (it_{2,\alpha} (\delta' \cdot \hat{\mathbf{x}}) e^{i\mathbf{A}\cdot\delta'_a} c_{i,a,\sigma}^+ c_{i+\delta'_a,a,\sigma} - H.c.)
\end{aligned} \tag{5}$$

The expectation value of the term in J proportional to A gives the total oscillator strength, $S(\infty) = \frac{2}{\pi} \int_0^\infty d\omega \sigma_1(\omega)$ in the conduction band contribution to the optical conductivity (see^{6,21,23} for details). Restoring units we have (a is the $Fe - Mo/Re$ distance, the sum rule is conventionally defined in terms of the conductivity per unit volume and the factor of two comes from the xy and xz orbitals, whose contributions to the expectation values are identical in cubic symmetry)

$$\begin{aligned}
S(\infty) = & \frac{2e^2}{a} \left\langle \sum_{i,\pm\delta_x,\sigma} (t_{1,a} c_{xy,i,\sigma}^+ c_{xy,i+\delta_x,\sigma} + H.c.) \right\rangle \\
& + \left\langle \sum_{i\in B',\delta'_a} (t_{2,\alpha} c_{i,a,\sigma}^+ c_{i+\delta'_a,a,\sigma} + H.c.) \right\rangle
\end{aligned} \tag{6}$$

The conductivity is

$$\sigma(\Omega) = \frac{S(\infty) - 2\chi_{jj}(\Omega)}{i\Omega} \tag{7}$$

with χ_{jj} the usual Kubo formula current-current correlation function evaluated using $J_x(A=0)$ (Eq 5) and again the factor of two represents the orbital degeneracy.

III. METHOD OF EVALUATION

A. Overview

To evaluate the properties of H we use the dynamical mean field method^{1,8} This method is extensively described and justified elsewhere, and is relevant here because the principal interactions are local. In brief the central approximation is that the electron self energy, Σ , is momentum independent. In this circumstance the physics may be derived from a local theory which may be viewed as a quantum impurity model combined with a self consistency condition. The application to the double perovskite systems requires some discussion. In these systems the unit cell contains two sites, each site contains three orbitals and there are two choices of spin, so the local theory has twelve degrees of freedom. However, the problem may be simplified. First, the three orbitals (d_{xy} etc) are coupled only via the interaction. Second, the interaction exists only on the Fe site, so that we may formally integrate out the electrons on the non- Fe (B') site, defining a single-orbital model with the inverse Fe (B)-site Green function for e.g. the xy orbitals viz

$$G_{BB}^{xy,band}(p,\omega)^{-1} = \omega - \frac{4t_1^2 (\cos(p_x) + \cos p_y)^2}{\omega + \Delta^{xy} - 4t_2(\cos(p_x) \cos(p_y))} \tag{8}$$

We measure momenta in units of π/a where $a \approx 4\text{\AA}$ is the distance from a B to a nearest neighbor B' site. The two dimensional Brillouin zone is defined by $|p_x + p_y| < \pi$.

The physics is then described by a three-orbital local theory given by the partition function $Z_{loc} = \int \mathcal{D}c^+ c \exp[S_{loc}]$ with an action S_{loc} which we write in the Matsubara frequency representation as

$$S_{loc} = T \sum_{\omega} Tr [c_{a\alpha}^+(\omega) (\mathbf{a}_{\alpha\beta}^{ab}(\omega) - \mathbf{J}\mathbf{S} \cdot \sigma_{\alpha\beta}) c_{a\beta}(\omega)] \tag{9}$$

involving fields $c_{a\alpha}$ and specified by a tensor mean field function \mathbf{a} which has orbital (ab) and spin ($\alpha\beta$) indices (the trace is over the spin and orbital indices). The mean field function is fixed by the condition that the Green function defined from S_{loc} ,

$$\mathbf{G}_{loc}(\tau) = \frac{\delta \ln Z_{loc}}{\delta \mathbf{a}(\tau)} = (\mathbf{a} - \Sigma)^{-1} \tag{10}$$

is equal to the local Green function defined by integrating Eq 8 over momenta using the self energy defined by Eq 10 i.e.

$$G_{loc}^{xy}(\omega) = \int \frac{d^2p}{(2\pi)^2} G_{BB}^{xy,band}(p, \omega - \Sigma) \tag{11}$$

and the integral is over the Brillouin zone defined above.

Substitution of Eqs 9 10 into Eq 11 yields explicit equations which are solved numerically by iteration.

B. Calculation of T_c

We calculate the ferromagnetic transition temperature by decomposing the mean field function \mathbf{a} into non-magnetic (a_0) and magnetic (a_1) parts

$$\mathbf{a} = a_0^a + a_1^a \mathbf{m} \cdot \sigma \tag{12}$$

and linearizing in a_1 . We take the magnetization direction \mathbf{m} to be parallel to z and take the limit $J \rightarrow \infty$ so that after integrating out the fermions and redefining $a \rightarrow a + J$ we obtain ($\cos(\theta)$ is the dot product between the direction of the core spin and of the magnetization)

$$S_{imp} = Tr \ln [a_0^a(\omega) + a_1^a(\omega) \cos(\theta)] \tag{13}$$

where the Tr is over the frequency index and the orbital degree of freedom.

The Green function of the impurity model becomes

$$G_{imp}^a(\omega) = \frac{1}{2} \left\langle \frac{1 - \hat{S} \cdot \vec{\sigma}}{a_0 - a_1 \cos(\theta)} \right\rangle \tag{14}$$

where the expectation value is over the directions of the 'core spin' S .

In the paramagnetic phase $a_1 = 0$. Expanding near the magnetic transition (assumed second order) yields

$$G^{imp}(\omega) = \frac{1}{2a_0} \left(1 - \left(m + \frac{a_1}{3a_0} \right) \sigma_z \right) \quad (15)$$

with $m = \langle \cos \theta \rangle$ so that

$$\Sigma(\omega) = -a_0 - \left(2a_0 m - \frac{a_1}{3} \right) \sigma_z \quad (16)$$

At $T > T_c$ $m = a_1 = 0$ and substitution of Eqs 16, 15 into Eq 11 yields

$$\frac{1}{2a_0(\omega)} = I_1(\omega, a_0(\omega)) \quad (17)$$

where the n^{th} order integral I_n is given by

$$I_n = \int \frac{d^2 p}{(2\pi)^2} (G_{22}(\omega))^n \quad (18)$$

This equation is solved numerically by iteration for a sufficiently dense set of frequency points (typically frequency spacing $0.04t_1$). Once a solution for a_0 is obtained we may linearize Eq 11 in the magnetic part of the self energy and local Green function, obtaining

$$\frac{m}{2a_0} - \frac{a_1}{6a_0^2} = I_2(\omega, a_0(\omega)) \left(2a_0 m + \frac{a_1}{3} \right) \quad (19)$$

where

$$m = \langle \cos \theta \rangle = \sum_{\omega, a} \frac{a_1^a}{3a_0^a} \quad (20)$$

Solving for a_1 and then using this to obtain an expression for m yields a self consistent equation for T_c which in the limit of cubic symmetry becomes

$$1 = \sum_n \frac{1 - 4a_0^2 I_2}{1 + 2a_0^2 I_2} = \sum_n \left[-2 + \frac{9}{1 + 2a_0^2 I_2} \right] \quad (21)$$

It turns out that the transition temperatures are low compared to the other scales of the model so that that one may recast this equation via analytical continuation to the real axis as (μ is the chemical potential corresponding to the desired carrier density)

$$T_c = \int_{-\infty}^{\mu} \frac{d\omega}{\pi} \text{Im} \left[\frac{9}{1 + 2a_0^2 I_2} \right] \quad (22)$$

IV. RESULTS AND DISCUSSION

We have calculated the magnetic transition temperature from Eq. 22, finding that for the parameters used to construct Fig. 1 (and which are the ones following from band theory) $n = 1$ (Re case) $T_c \approx 110K$ and that

for $n = 2$ (*Mo* case) the ground state is not ferromagnetic. These calculated values are in sharp disagreement with the experimental values $T_c \gtrsim 400K$ for both $n = 1$ and $n = 2$. The relatively small values of T_c found for $n = 1$ in this calculation may be understood from the density of states, which shows that the low-lying states lie mainly on the *non-Fe* sites, which are far displaced in energy from the magnetic site and therefore do not hybridize strongly with it, so the effective carrier-spin interaction is not strong. That the $n = 2$ is non-magnetic may be understood by combining the results of⁸ with the observation that the band structure is effectively two dimensional. In the extreme weak coupling limit, the nature of the magnetic ground state is determined by the wave vector at which the susceptibility is maximal. For the two dimensional band structures considered here this maximum is not at $q = 0$. Ref⁸ showed that in the DMFT approximation, increasing the carrier-spin coupling increased the range in which ferromagnetism existed, but that as band filling is increased, a transition to an antiferromagnetic state generically occurs, and gets pushed to the half-filled band only for J of the order of the bandwidth. These effects are more pronounced for the two dimensional band structure we consider.

The relative weakness of the virtual *Re/Mo* \leftrightarrow *Fe* transitions is reflected in the temperature dependence of the many-body density of states, shown for the 'band' parameters in the lower panel of Fig. 1. Comparing these we see that disordering the *Fe* spins leads to a slight narrowing of the bands, but the larger (30%) band narrowing effects found in *CMR* manganites⁷ are not observed for these parameters.

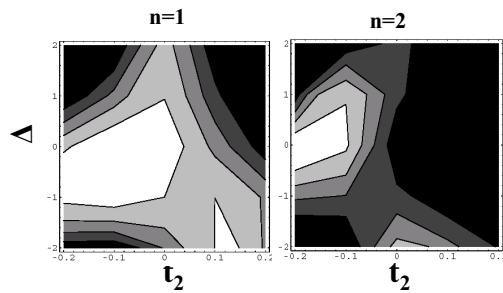


FIG. 3: *Left panel:* Contour plots of calculated transition temperatures for range of model parameters and conduction band density $n = 1$. *Right panel:* Contour plots of calculated transition temperature for $n = 2$. In each figure, contours are spaced approximately 100 Kelvin apart and the white areas correspond to transition temperatures in excess of 400K.

To understand the behavior of the model in more detail we have evaluated the predicted ferromagnetic transition temperatures for wide range of model parameters. The results are summarized in the two panels of Fig. 3 which

show via contour plots the values of T_c predicted by the method. The contours are spaced approximately $100K$ apart, and the black regions indicate the areas in which the calculated T_c vanishes. It is seen that in order to obtain a reasonably high transition temperature, especially for the $n = 2$ band filling, one must choose the parameter t_2 to have the opposite sign from the physical one. The reason for this behavior is revealed by Fig. 2, which shows the density of states for parameters which maximize the $n = 2$ T_c . The low-lying states for this case are seen to be of mainly *Fe* character, because the level repulsion argument which pushed down the non-*Fe* states for the LSDA parameters is not operative here.

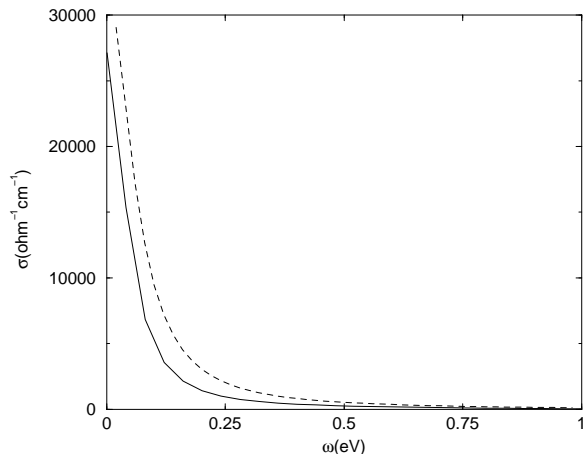


FIG. 4: $T = 0$ (dashed) and $T > T_c$ conductivities for $n = 1$ using best-fit band parameters $t_1 = 0.25eV$, $t_2 = 0.15eV$, $t_3 = 0.03eV$ and $\Delta = 0.3eV$ used in Fig. 1. The $T = 0$ conductivity was computed using an artificial broadening of $0.1eV$ applied to the *B* site.

We have also calculated the optical conductivity for various model parameters. Results obtained using the LSDA parameters are shown in Figs. 4 (*Re*-case, $n = 1$) and fig. 5 (*Mo*-case, $n = 2$). One would in principle expect two classes of transitions: a 'Drude' peak centered at $\omega = 0$ involving motion of electrons near the Fermi surface and an interband transition involving moving an electron from a *Re/Mo* to a *Fe*. Our calculations indicate that for the tight binding parameters corresponding to the LSDA calculation, the interband feature is very weak, indeed not visible in the Figure again demonstrating the weakness of the *Fe* – *Mo* coupling for these parameters. We observe that the 'Drude' part has a distinctly non-Drude form, which arises because in our calculation the scattering processes couple to the 'B' (*Fe*) site only; although the regions of momentum space where the hybridization vanishes are of measure zero, they do lead to a frequency dependence of the scattering rate which explains the peculiar form. We also note that the main cause of the changes in conductivity and oscillator strength between $T = 0$ and $T = T_c$ is the change in band filling, which leads to a change in optical matrix

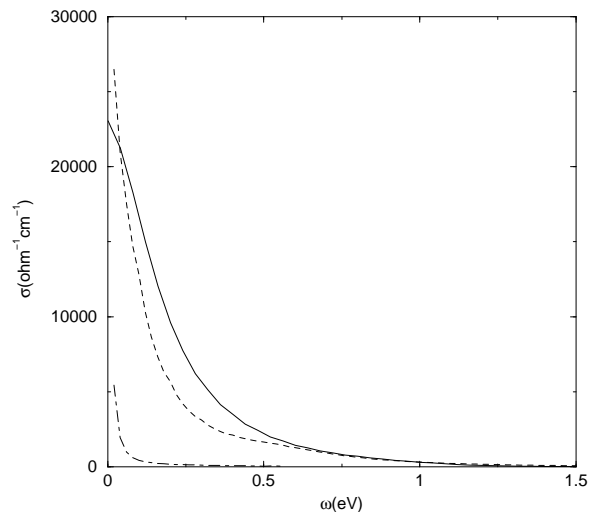


FIG. 5: Upper panel: $T = 0$ (dashed) and $T > T_c$ (solid) conductivities for $n = 2$. using best-fit band parameters $t_1 = 0.25eV$, $t_2 = 0.15eV$, $t_3 = 0.03eV$ and $\Delta = 0.3eV$ used in Fig. 1. The $T = 0$ conductivity was computed using an artificial broadening of $0.1eV$ applied to the *B* site. The small contribution to the $T = 0$ conductivity arising from the minority spin band is shown as the dash-dot line.

element. In the paramagnetic state one has three bands, each with a two-fold spin degeneracy, corresponding to a filling of $n/6$ ($n=1,2$ is the particle density), so the relevant states are quite close to the bottom of the band where the optical matrix element is small. In the ferrimagnetic state for $n = 1$ one loses the spin degeneracy, so one has three bands each filled to a higher level, so with a correspondingly higher Fermi velocity and optical matrix element, whereas for the $n = 2$ case the temperature induced shift corresponds to a change from $1/3$ to $2/3$ filled band, with much smaller change in optical matrix elements. The temperature dependent change in the oscillator strength is therefore much less. As noted above, in the ferrimagnetic case for $n = 2$ one has a small filling of the majority spin band, leading to a small additional contribution to σ , shown as the dot-dashed line in Fig. 5.

The conductivity corresponding to the parameters which maximize T_c (Fig 2) is shown in Fig. 6. We see that the different electronic structure leads to a different optical conductivity: the Drude absorption is weaker, and a peak corresponding to excitation of carriers from *Fe* to *Re/Mo* is evident.

The conductivity of Sr_2FeMoO_6 has been measured by Jung and co-workers²⁴. These authors found a conductivity which was of roughly the Drude form, (albeit with a rather larger scattering rate than we have used) but additionally has a weak kink at a frequency of approximately $0.6eV$. It is interesting to speculate that this kink is a signature of the 'interband' feature which we found only for the 'antiphysical' parameters. A more detailed experimental investigation of the band structure

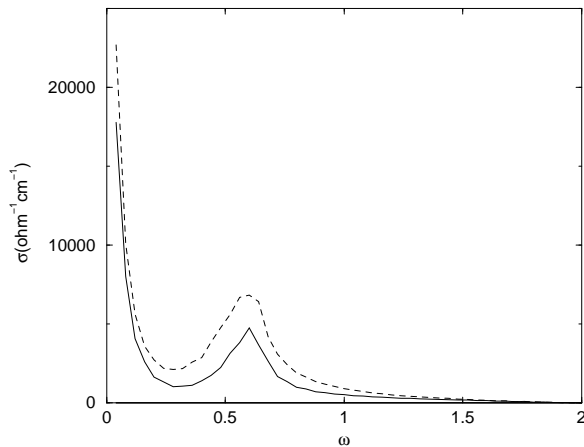


FIG. 6: $T = 0$ (dashed) and $T > T_c$ (solid) optical conductivities for $n = 1$ and band parameters $t_1 = 0.25eV$, $t_2 = -0.15eV$ and $\Delta = 0$ corresponding to the density of states shown in Fig 2.

may be warranted.

V. CONCLUSIONS

We have used the dynamical mean field method to determine the ferromagnetic transition temperature, density of states and optical conductivity of a model representing key physics (two dimensionality of band structure and strong on-site interaction on Fe site) of the double perovskite ferrimagnets $Sr_2Fe(Mo/Re)O_6$. Our method can easily be generalized to include the effects of mis-site

disorder, or lattice distortions which split the t_{2g} levels. However, such generalization is not immediately warranted because the calculated transition temperatures are, at least for the parameters following from band structure calculations, in qualitative disagreement with experimental data—in particular, the calculation predicts that Sr_2FeMoO_6 is not ferrimagnetic, whereas experiment indicates that it is with a T_c in excess of $400K$, and under-predicts the T_c of Sr_2FeReO_6 by a factor of almost 4.

The essential reason for this was found to be that the band theory parameters imply that the mobile carriers reside mainly on the *non-Fe* sites, and hybridize weakly with these sites. Optical conductivity signatures of the weak hybridization were demonstrated. The calculation indicates that transition temperatures would be substantially raised if parameters are used for which the added carriers are largely on the Fe sites. An alternative possibility is that an interaction omitted from the model is crucially important; in particular that the magnetism should not be regarded as arising from correlations on the Fe site, but should instead be thought of more as a Stoner instability of the band arising from the Re/Mo states. The additional interaction proposed in¹⁵ would tend to produce this physics and an important next step would be to extend the methods developed here to the treatment of this case.

Acknowledgements: This work was supported by the University of Maryland/Rutgers MRSEC (AJM and AC) and NSF-DMR-00081075 (KP) and DARPA contract no. DAAD19-01-C-0060 (AC). We thank B. G. Kotliar, S. Ogale, H.D. Drew, B. A. Jones and S. Cheong for helpful conversations.

-
- ¹ A. Georges, B. G. Kotliar, W. Krauth and M. J. Rozenberg, Rev Mod Phys **68** 13-113 (1996).
 - ² N. Furukawa, J. Phys. Soc. Jpn. **64** 2734 (1995).
 - ³ A. Chattopadhyay, S. Das Sarma and A. J. Millis, Phys. Rev. Lett. **87** 227202/1-4 (2001).
 - ⁴ E. Hwang, A. J. Millis and S. Das Sarma, Phys. Rev. **B65** 233206/1-4 (2002).
 - ⁵ A. I. Liechtenstein, M. Katsnelson and B. G. Kotliar, Phys. Rev. Lett. **87** 067205/1-4 (2001).
 - ⁶ M. Quijada, J. Cerne, J. R. Simpson, H. D. Drew, K-H. Ahn, A. J. Millis, R. Shreekala, R. Ramesh, M. Rajeswari and T. Venkatesan, Phys. Rev. **B58** 16093-102 (1998).
 - ⁷ A. J. Millis, R. Mueller and B. I. Shraiman, Phys. Rev. **B54** 5406 (1996).
 - ⁸ A. Chattopadhyay, A. J. Millis and S. Das Sarma, Phys. Rev. **B61** 10738-49 (2000).
 - ⁹ A W Sleight, J. M. Longo and R. Ward, Inorg. Chem **1** 245 (1962).
 - ¹⁰ K. I. Kobayashi, T. Kimura, Y. Tomioka, H. Sawada, K. Terakura and Y. Tokura, Phys. Rev. **B59** 11159-62 (1998).
 - ¹¹ K. I. Kobayashi, T. Kimura, H. Sawada, K. Terakura and Y. Tokura, Nature **395** 677 (1998).
 - ¹² D. D. Sarma, P. Mahadevan, T. Saha-Dasgupta, S. Ray and A. Kumar, Phys. Rev. Lett. **85** 2549-52 (2000).
 - ¹³ J. Gopalakrishnan, A. Chattopadhyay, S. B. Ogale, T. Venkatesan, R. L. Greene, A. J. Millis, K. Ramesha, B. Hannoyer and G. Marest, Phys. Rev. **B62** 9538-42 (2000).
 - ¹⁴ A. Chattopadhyay and A. J. Millis, Phys. Rev. **B64**, 024424/1-4, (2001).
 - ¹⁵ S. Ray, A. Kurnar, D.D. Sarma, R. Cirino, S. Turchini, S. Zennaro and N. Zema, Phys. Rev. Lett. **87** 097204/1-4 (2001).
 - ¹⁶ C. Tang et. al., IEE Trans. magn. **35** 2574 (1999).
 - ¹⁷ W. Black and B. Das, A. Appl. Phys. **87** 6674 (2000).
 - ¹⁸ see, e.g. S. Das Sarma, "Spintronics" american Scientist **89** 516 (2001) and S. Das Sarma, J. Fabian, X. Hu, and I. Zutic, "Spin electronics and spin computation", Solid State Commun. **119**, 207 (2001).
 - ¹⁹ For a comprehensive review of recent work on 'correlated' transition metal oxides see e.g. M. Imada, A. Fujimori and Y. Tokura, Rev. Mod. Phys. **70** 1039 (1998)
 - ²⁰ for a detailed discussion of the calculated band theory and experimental fermi surface of a $4d$ transition metal oxide see C. Bergemann, S. R. Julian, A. P. Mackenzie, S. Nishizawa and y. Maeno, Phys. Rev. Lett. **84** 2662-6 (2000).

- ²¹ P. F. Maldague, Phys. Rev. **B16** 2437 (1977).
- ²² K. Ahn and A. J. Millis, Phys. Rev. **B61** 13545-559 (2000) and **B63** 209902 (2001) (E).
- ²³ A. J. Millis, Journal of Electron Spectroscopies and Related Phenomena (Netherlands) **114-116**, 669-78, (2001).
- ²⁴ J. H. Jung et. al., Phys. Rev. **B66** 104415-1/7 (2002).